SAND2017-2113J

Enhanced dielectric and piezoelectric responses in $Zn_{1-x}Mg_xO$ thin films near the phase separation boundary

Xiaoyu Kang[1], Smitha Shetty[2], Lauren Garten[2], Jon F. Ihlefeld[3], Susan Trolier-McKinstry[2] and Jon-Paul Maria[1]

[1]*Department of Materials Science and Engineering, North Carolina State University, Raleigh, North Carolina, 27695, USA*

[2]*Department of Materials Science and Engineering and Materials Research Institute, Pennsylvania State University, University Park, Pennsylvania, 16802, USA*

[3]*Electronic, Optical, and Nano Materials Department, Sandia National Laboratories, Albuquerque, New Mexico, 87185, USA*

Dielectric and piezoelectric properties for $Zn_{1-x}Mg_xO$ (ZMO) thin films are reported as a function of MgO composition up to and including the phase separation region. $Zn_{1-x}Mg_xO$ ($0.25 \leq x \leq 0.5$) thin films with *c*-axis textures were deposited by pulsed laser deposition on platinized sapphire substrates. The films were phase pure wurtzite for MgO concentrations up to 40%; above that limit, a second phase with rocksalt structure evolves with strong {100} texture. With increasing MgO concentration, the out-of-plane ($d_{33,f}$) and in-plane ($e_{31,f}$) piezoelectric coefficients increase by 360% and 290% respectively. The increase in piezoelectric coefficients is accompanied by a 35% increase in relative permittivity. Loss tangent values fall monotonically with increasing MgO concentration, reaching a minimum of 0.001 for $x \geq 0.30$, at which point the band gap is reported to be 4 eV. The enhanced piezoelectric response, the large band gap, and the low dielectric loss make $Zn_{1-x}Mg_xO$ an interesting candidate for thin film piezoelectric devices, and demonstrate that compositional phase transformations provide opportunities for property engineering.

Recent reports for AlN thin film actuators demonstrate a 400% enhancement in the longitudinal piezoelectric coefficient d_{33} by alloying with ScN over a composition range spanning the phase separation region.[1] Enhanced transverse piezoelectric constant e_{31}, electromechanical coupling factor k_t^2, and dielectric constant ε_{33} values were also measured for single phase ScN-AlN alloys.[2–4] Using first principle calculations, Tasnadi *et al.*[5] showed that softening of the wurtzite structure and flattening of free energy profile as a function of *c*/*a* ratio was responsible for the composition-dependent property trends.

It is interesting to consider whether such an effect is reserved to special cases, or is a general approach for property engineering. If the latter is true, opportunities may be present at "generic" composition-driven phase boundaries. In this context, generic refers to boundaries between materials that are as structurally dissimilar as wurtzite ZnO and rocksalt MgO. Considering how many phase boundaries are present in ternary and quaternary systems, this approach may be of some interest.

To address this question, the composition-dependent dielectric and piezoelectric properties of $Zn_{1-x}Mg_xO$ (ZMO) are investigated in the region approaching phase separation. Similar to $Al_{1-x}Sc_xN$, its structural end-members are wurtzite (polar) and rock salt (nonpolar) phases. The MgO-ZnO system was explored extensively by the wide band gap semiconductor community, motivated by the potential for efficient ultraviolet light emitting diodes. During their investigations, they showed that up to 50 mol.% MgO can dissolve in ZnO and the band gap is tunable between 3.3 eV and 4.5 eV.[6–8] From the perspective of a piezoelectric or dielectric application this is an appealing trend considering that the band gap will be large in compositions where the electromechanical response is potentially largest. We note that $Zn_{1-x}Mg_xO$ was first proposed as a piezoelectric material by Emanetoglu *et al.*[9] in 2003 motivated by the desire for increased acoustic wave velocity. They demonstrated ZMO actuators in surface and bulk acoustic wave devices.[9–13] However, composition-dependent property optimization and trends were not described, particularly those approaching phase separation.

The data in this letter demonstrate that the ZMO thin film piezoelectric coefficients exceed those of ZnO by 3X, up to compositions that approach phase separation. All films within this study were grown on platinized *c*-sapphire substrates using pulsed laser deposition (PLD). Platinum bottom electrodes were achieved with a ZnO adhesion layer using the method of Shelton *et al.*[14] $Zn_{1-x}Mg_xO$ targets were prepared from ZnO (Alfa Aesar, 99.9%) and MgO (Alfa Aesar, 99.99%) powders that were vibratory milled with ZrO_2 media, pelletized with uniaxial pressing, and sintered at 1300 °C in air with *x*-values spanning 0.25 to 0.50. To promote unipolar *c*-axis texture, all depositions began with a high temperature (440 °C) 10 nm buffer layer of ZnO as described by Liu *et al.*[15] Reports of unipolar ZnO on platinum surfaces are also available in the literature.[16,17] Following preparation of this seed layer, the substrate was maintained at the same temperature, and deposition was switched to an alloy target with the desired MgO content. Target exchanges were performed without breaking vacuum. For both buffer layer and alloy film depositions, the ceramic targets were ablated with KrF excimer laser radiation with a fluence of 3.8 J/cm^2 and repetition rate of 10 Hz. The substrate to target distance was 6.5 cm. The oxygen pressure for ZnO buffer layer and $Zn_{1-x}Mg_xO$ films were 10^{-4} Torr and 20 mTorr, respectively. The film thickness was typically around 500 nm. Substrate rotation and laser beam raster on the targets were performed to further improve film thickness uniformity. $Zn_{1-x}Mg_xO$ thin films were annealed subsequently in a tube furnace in flowing oxygen ambient at 700 °C for 2 hours; this anneal is necessary to reduce dielectric dispersion, presumably by promoting oxygen uptake.

MgO contents reported below refer to those of the ceramic targets. The actual film compositions may be slightly higher due to the volatility of ZnO and Zn.[8]

The crystal structure and surface morphology were investigated with X-ray diffraction (XRD – Panalytical Empyrean, parallel beam optics), field emission scanning electron microscopy (FESEM – FEI Verios 460L) and atomic force microscopy (AFM – Asylum Research). Parallel plate capacitor structures were made by patterning sputtered platinum with a lift-off process. Top contacts were squares with a side length of 300 μm – this dimension was chosen so that the capacitor width is similar to the substrate thickness (330 μm).[18] Dielectric properties were measured with LCR meter (HP4192A) in the frequency range of 1 kHz to 10 MHz. For piezoelectric measurements, double beam laser interferometry (AixACCT DBLI)[19] and the wafer flexure method[20] were used for longitudinal and the transverse piezoelectric coefficients, respectively.

Initial structural characterization with X-ray diffraction was used to determine phase, to infer composition, and to measure lattice constant trends with Mg incorporation. Fig. 1 shows a summary of the X-ray diffraction data from which several conclusions can be drawn: 1) MgO additions up to 35% produce single phase wurtzite material with the out-of-plane (0002) reflection shifting to lower 2θ values indicating an increasing lattice constant; 2) between 35% and 40% MgO, a second phase with diffraction peaks consistent with a rocksalt structure is observed; as expected the lattice parameter of the wurtzite is constant in the two-phase region up to 48% MgO; 3) The wurtzite phase is uniformly *c*-axis oriented for all compositions; and 4) after phase separation, the rocking curve widths increase and the wurtzite peak intensities fall – both consistent with increasing disorder and mosaicity. It is noted that the X-ray data in Fig. 1 were collected from the annealed films – additional measurements (not shown) show no appreciable differences in the as-grown state.

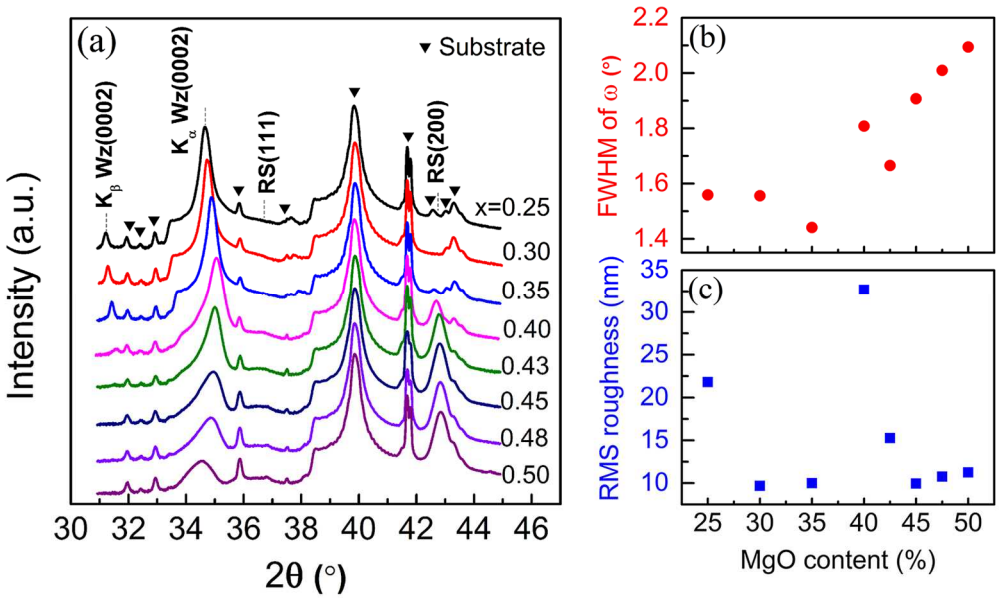

FIG. 1. X-ray diffraction of 2θ-ω scan (a), rocking curve FWHM of wurtzite (0002) (b) and RMS roughness (c) of $Zn_{1-x}Mg_xO$ ($0.25 \leq x \leq 0.5$) annealed thin films. RS = rocksalt, while Wz denotes the wurtzite structure. Between approximately 35% and 48% MgO (the phase separated

region), the wurtzite out of plane lattice parameter is constant. RMS roughness was measured by AFM at regions of 5μm × 5μm.

SEM analysis of film morphology in the wurtzite region revealed ~100 nm grains for the 25% MgO sample, and a modest trend of decreasing grain diameter with increasing MgO. The SEM images in Fig. 2 show representative images for MgO contents between 25% and 50%. At the 40% MgO sample, two morphology types are present that are likely associated with the two phases, rocksalt and wurtzite, that are present in XRD spectra. None of the SEM images suggest the presence of film cracking. AFM analysis shows that surface roughness is largest for compositions just after the onset of multiple phases, which, for the 40% MgO film was 30 nm RMS. At 50% MgO, the film microstructure exhibited a morphology characterized by clusters of very tiny grains. Such very small grains are consistent with other MgO films prepared by PVD.[21]

It is important to determine if film polarity is uniform and homogeneous for all compositions. To test polarity, several ZMO films with different MgO contents were SEM imaged before and after etching in 0.3 M HCl. There was no evidence of strong etching anisotropy, which would be expected for mixed polarity.[22] We note, in addition, that the polarity determining step, the 10 nm high temperature ZnO buffer layer, is the same for all film compositions.

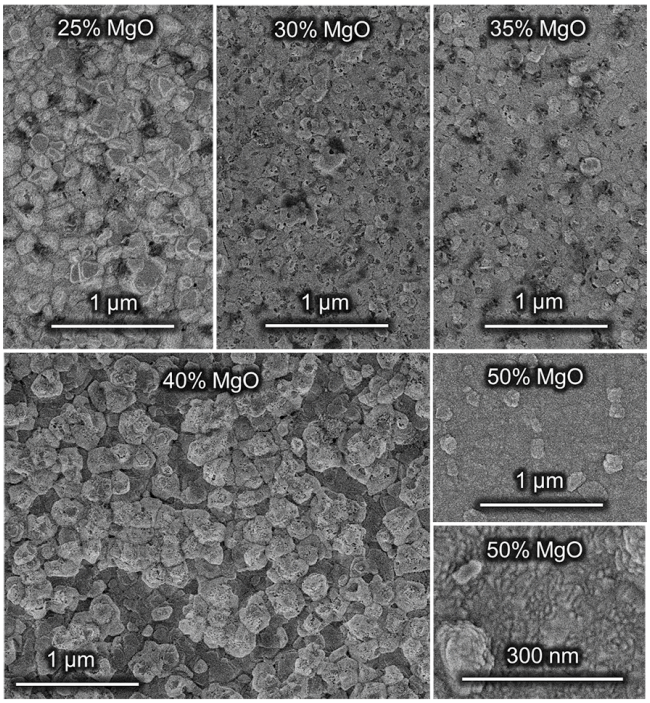

FIG. 2. FESEM morphology of $Zn_{1-x}Mg_xO$ thin films with MgO contents between 25% and 50%. From 25% to 35% MgO, the grain size exhibits a small reduction. At 40% MgO two populations of grains emerge which likely correspond to rocksalt crystalline phase observed by X-ray diffraction.

Fig. 3 gives the frequency dependent dielectric properties for the $Zn_{1-x}Mg_xO$ ($0.25 \leq x \leq 0.5$) thin film series. From 3 kHz to 4 MHz, relative permittivity exhibits a modest frequency dependence in all compositions. The 25% MgO thin film shows the highest loss and dispersion, which is

likely associated with it having the smallest band gap and strongest propensity for oxygen loss. For all other samples loss tangent values are below 0.007 in the frequency range not affected by the onset of fixture resonance. Note that the sharp increase occurring above 1 MHz results from approaching resonance of the measurement system.

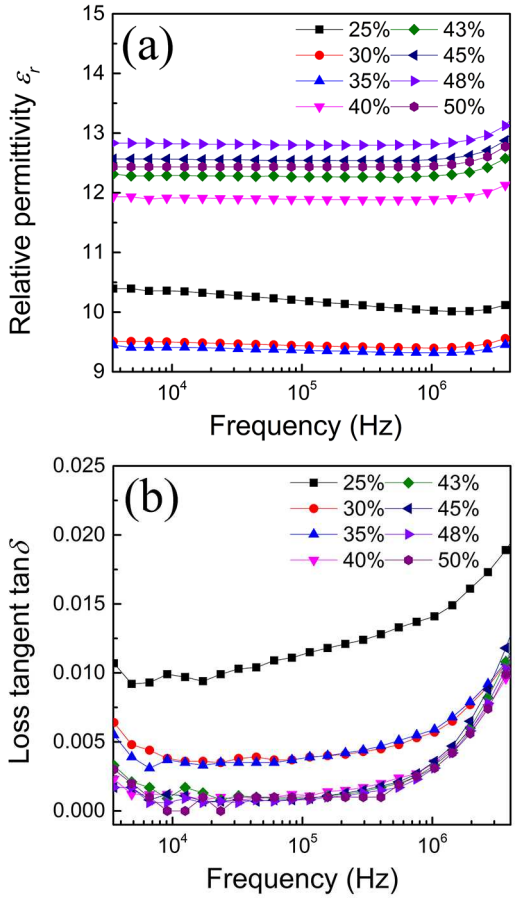

FIG. 3. Relative permittivity (a) and loss tangent (b) of $Zn_{1-x}Mg_xO$ thin films with MgO contents between 25% and 50% at 3 kHz to 4 MHz.

To better visualize the composition trends, Fig. 4 provides a summary of the dielectric constant and loss tangent data as a function of MgO content. Each data point is a value averaged over the entire frequency range. For MgO compositions in the wurtzite phase all films exhibit a *c*-axis permittivity (ε_{33}) around 9.5, the higher value at 25% MgO is likely associated with a larger dielectric loss because of the lower MgO concentration. At the phase separation boundary between 35% and 40% MgO, there is an abrupt increase to a value ~ 11.9 with, perhaps, a broad maximum at ~ 48% MgO. In this region, since multiple phases are present, only an effective value can be reported. This abrupt change of permittivity was observed previously by Bundesmann *et al.*, and attributed to an increase in bond polarizability that accompanies the change from four-fold to six-fold coordinated metal cations at the phase separation region.[23] It is also possible that a flatter energy profile, which has been proposed to explain higher piezoelectric coefficient d_{ij} values in such materials near a phase transition, could also contribute to the ionic polarizability. It is interesting to note that while the loss tangent values for all Zn_{1-}

$_x$Mg$_x$O thin films reported in Fig. 4 are ≤ 0.01, for samples with greater than 30% MgO, tan δ is ~ 0.004 or lower, a value range comparable to pure AlN thin films.[3] The leakage current of Zn$_{1-x}$Mg$_x$O thin films generally decrease with MgO content from 1×10^{-3} A/cm^2 at 25% Mg to 1×10^{-8} A/cm^2 at 50% Mg under field strength of 100 kV/cm. These loss tangent and leakage current reductions are consistent with a larger band gap.[6–8]

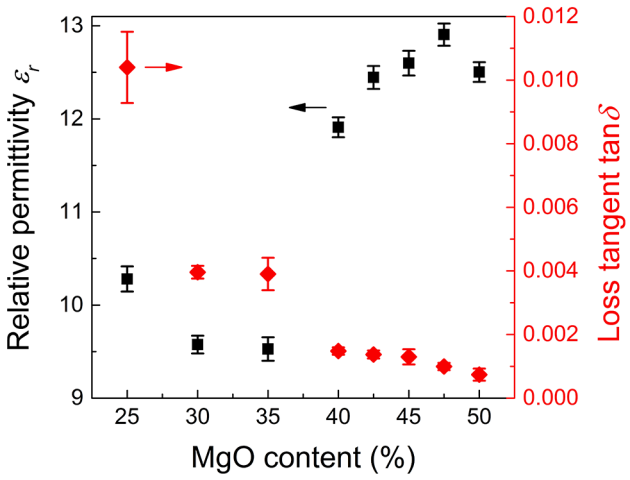

FIG. 4. Relative permittivity and loss tangent of Zn$_{1-x}$Mg$_x$O ($0.25 \leq x \leq 0.5$) thin films as a function of MgO content. Data points are averaged from 3 kHz to 4 MHz.

In-plane and out-of-plane piezoelectric measurements were performed to identify composition trends in the electromechanical response. Fig. 5 shows a summary of data for the constrained longitudinal and transverse piezoelectric coefficients $d_{33,f} = e_{33}/c_{33}^E$ and $e_{31,f} = d_{31}/(s_{11}^E + s_{12}^E)$.[24] An enhanced response in both longitudinal and transverse direction is present near the phase boundary, with nearly identical composition dependence. Maximum values for $d_{33,f}$ and $e_{31,f}$ are 10.8 pm/V and -1.4 C/m^2, and occur for the 35% MgO composition. Relative to the lowest MgO contents explored in this data set, these values represent increases of 360% and 290%, respectively. After phase separation, both piezoelectric coefficients decrease quickly. Within a few mol.% MgO, the piezo-response is within the measurement noise. This is consistent with X-ray diffraction patterns in Fig. 1 which show substantial rocksalt fractions and a significant mosaicity for the remaining wurtzite. In the context of other literature reports, the values found for 35% MgO remain interesting. Carlotti et al.[25] reported some of the highest piezo-coefficients available, for thick (*i.e.*, 3 µm to 17 µm) epitaxial ZnO films on sapphire. In their work, e_{31} values of -0.51 C/m^2 were found. The maximum values reported presently, for much thinner samples with a lower thermal budget, and a stronger mosaic structure are more than 2X larger.

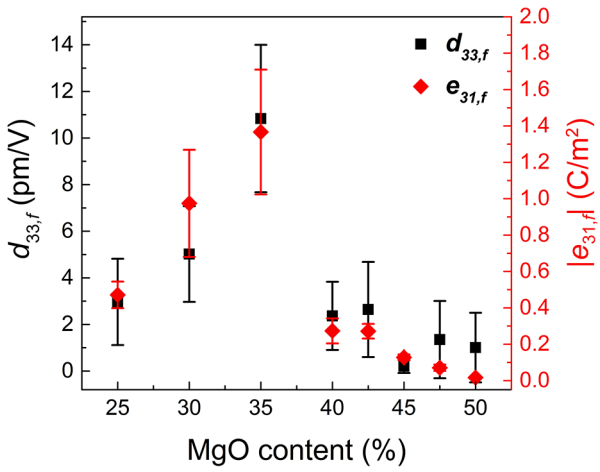

FIG. 5. Longitudinal and transverse piezoelectric coefficient $d_{33,f}$ and $e_{31,f}$ of $Zn_{1-x}Mg_xO$ ($0.25 \leq x \leq 0.5$) thin films.

The present trend in piezo-response is analogous to that in the $Sc_xAl_{1-x}N$ system, however, the composition range over which this occurs is narrower and in tight proximity to the phase boundary. Furthermore, property enhancements are confined exclusively to the single-phase region. It is important to note that the *c/a* ratio values of wurtzite $Zn_{1-x}Mg_xO$ thin films are all close to 1.6, which are consistent with Ohtomo *et al.*[8] As such, there is no structural data suggesting the presence of the metastable hexagonal MgO phase, which has a theoretical *c/a* of 1.2.[26] The authors hypothesize that the enhancement in $Zn_{1-x}Mg_xO$ piezoelectric coefficients can be attributed to an elastic softening effect similar to that used to explain the composition trends in $Sc_xAl_{1-x}N$.[5] By analogy, this model would suggest that MgO concentrations close to phase separation lead to competition between tetrahedral and octahedral cation coordination and a similarly frustrated system with reduced elastic constants and flattened energy profile that increases sensitivity to external strain. Due to the lack of an intermediate metastable phase (i.e. hexagonal MgO) one would not expect a saddle point on the energy profile connecting the wurtzite and rocksalt phases and by comparison to $Sc_{0.5}Al_{0.5}N$, a flattened profile more centered to the wurtzite phase.[5] We speculate that this particular energy profile shape is consistent with piezoelectric enhancement exclusive to single phase region in $Zn_{1-x}Mg_xO$ thin films. In addition, without assistance from a metastable phase, $Zn_{1-x}Mg_xO$ system would be a more generic example to the concept from Damjanovic[27] that property enhancement widely exists at phase transition boundary with easy polarization extension or contraction pathways between polar and non-polar phases, due to a flattened free energy landscape as a function of *a*- and *c*-axis components of polarization.

In conclusion, a series of $Zn_{1-x}Mg_xO$ thin films were prepared by PLD with varying MgO content. The thin films exhibited enhanced piezoelectric response in the vicinity of phase separation. We found 360% and 290% enhancements of $d_{33,f}$ and $e_{31,f}$ piezoelectric coefficients respectively when $x = 0.35$. Moreover, addition of Mg reduces significantly tan δ to the order of 10^{-3}, which is comparable to AlN. From all the investigated MgO compositions, $Zn_{0.65}Mg_{0.35}O$ has optimized piezoelectric response with low dielectric loss. The composition modification producing this enhanced piezo-response boosts the bandgap to > 4 eV, as inferred by known trends between measured lattice constant, MgO content, and bandgap.[6–8] This is in contrast to

$Sc_xAl_{1-x}N$, where Sc additions lower the bandgap to 2.5 eV at maximum d_{33}.[28] It is conceivable that stronger enhancements are possible if additional Mg could be stabilized in the hexagonal phase using better lattice matched substrates or different deposition methods.[6,7] Most importantly, we speculate that the concept of a flattened energy landscape may be applied more broadly among materials in proximity to a composition-driven phase transitions, providing expanded opportunities for property engineering.

This work was supported by the NSF Center for Dielectrics and Piezoelectrics (NSF 1361503), and the Army Research Office contract (W911NF1410285). The authors acknowledge the use of the Analytical Instrumentation Facility (AIF) at North Carolina State University, which is supported by the State of North Carolina and the National Science Foundation.

[1] M. Akiyama, T. Kamohara, K. Kano, A. Teshigahara, Y. Takeuchi, and N. Kawahara, Adv. Mater. **21**, 593 (2009).

[2] R. Matloub, M. Hadad, A. Mazzalai, N. Chidambaram, G. Moulard, C.S. Sandu, Th . Metzger, and P. Muralt, Appl. Phys. Lett. **102**, 152903 (2013).

[3] G. Wingqvist, F. Tasnádi, A. Zukauskaite, J. Birch, H. Arwin, and L. Hultman, Appl. Phys. Lett. **97**, 112902 (2010).

[4] M. Moreira, J. Bjurström, I. Katardjev, and V. Yantchev, Vacuum **86**, 23 (2011).

[5] F. Tasnádi, B. Alling, C. Höglund, G. Wingqvist, J. Birch, L. Hultman, and I. a. Abrikosov, Phys. Rev. Lett. **104**, 137601 (2010).

[6] T. Takagi, H. Tanaka, S. Fujita, and S. Fujita, Jpn. J. Appl. Phys. **42**, L401 (2003).

[7] T. Minemoto, T. Negami, S. Nishiwaki, H. Takakura, and Y. Hamakawa, Thin Solid Films **372**, 173 (2000).

[8] A. Ohtomo, M. Kawasaki, T. Koida, K. Masubuchi, H. Koinuma, Y. Sakurai, Y. Yoshida, T. Yasuda, and Y. Segawa, Appl. Phys. Lett. **72**, 2466 (1998).

[9] N.W. Emanetoglu, A. Member, S. Muthukumar, P. Wu, R.H. Wittstruck, Y. Chen, and Y. Lu, IEEE Trans. Ultrason. Ferroelectr. Freq. Control **50**, 537 (2003).

[10] R.H. Wittstruck, X. Tong, N.W. Emanetoglu, P. Wu, Y. Chen, J. Zhu, S. Muthukumar, Y. Lu, and A. Ballato, IEEE Trans. Ultrason. Ferroelectr. Freq. Control **50**, 1272 (2003).

[11] Y. Chen, G. Saraf, R.H. Wittstruck, N.W. Emanetoglu, and Y. Lu, Proc. 2005 IEEE Int. Freq. Control Symp. Expo. 2005. 142 (2005).

[12] Y. Chen, P.I. Reyes, Z. Duan, G. Saraf, R. Wittstruck, Y. Lu, O. Taratula, and E. Galoppini, J. Electron. Mater. **38**, 1605 (2009).

[13] Y. Chen, G. Saraf, Y. Lu, L.S. Wielunski, and T. Siegrist, J. Vac. Sci. Technol. A Vacuum, Surfaces, Film. **25**, 857 (2007).

[14] C.T. Shelton, P.G. Kotula, G.L. Brennecka, P.G. Lam, K.E. Meyer, J.P. Maria, B.J. Gibbons, and J.F. Ihlefeld, Adv. Funct. Mater. **22**, 2295 (2012).

[15] Y.Z. Liu, M.J. Ying, X.L. Du, Z.Q. Zeng, Z.X. Mei, J.F. Jia, Q.K. Xue, and Z. Zhang, Phys. Lett. A **339**, 497 (2005).

[16] B.T. Khuri-Yakub, J.G. Smits, and T. Barbee, J. Appl. Phys. **52**, 4772 (1981).

[17] T. Nakamura, Y. Yamada, T. Kusumori, H. Minoura, and H. Muto, Thin Solid Films **411**, 60 (2002).

[18] S. Sivaramakrishnan, P. Mardilovich, a. Mason, a. Roelofs, T. Schmitz-Kempen, and S. Tiedke, Appl. Phys. Lett. **103**, 132904 (2013).

[19] W.Y. Pan and L.E. Cross, Rev. Sci. Instrum. **60**, 2701 (1989).

[20] R.H.T. Wilke, P.J. Moses, P. Jousse, C. Yeager, and S. Trolier-McKinstry, Sensors Actuators A Phys. **173**, 152 (2012).

[21] K.E. Meyer, R. Cheaito, E. Paisley, C.T. Shelton, J.L. Braun, J.P. Maria, J.F. Ihlefeld, and P.E. Hopkins, J. Mater. Sci. **51**, 1 (2016).

[22] H. Tampo, P. Fons, A. Yamada, K.K. Kim, H. Shibata, K. Matsubara, H. Yoshikawa, H.

Kanie, and S. Niki, Appl. Phys. Lett. **87**, 141904 (2005).

[23] C. Bundesmann, a. Rahm, M. Lorenz, M. Grundmann, and M. Schubert, J. Appl. Phys. **99**, 113504 (2006).

[24] S. Trolier-McKinstry and P. Muralt, J. Electroceramics **12**, 7 (2004).

[25] G. Carlotti, G. Socino, a. Petri, and E. Verona, Appl. Phys. Lett. **51**, 1889 (1987).

[26] S. Limpijumnong and W. Lambrecht, Phys. Rev. B **63**, 1 (2001).

[27] D. Damjanovic, Appl. Phys. Lett. **97**, 62906 (2010).

[28] R. Deng, S.R. Evans, and D. Gall, Appl. Phys. Lett. **102**, 112103 (2013).